SCIENTIFIC CULTURE
www.sci-cult.com

SCIENTIFIC CULTURE, Vol. 10, No. 2, (2024), pp. 1-13
Open Access. Online & Print

DOI: 10.5281/zenodo.10621731

TOWARDS CONSOLIDATION, EFFECTIVENESS AND COMPATIBILITY OF PAINTED LAYERS IN ANCIENT EGYPTIAN COFFIN BY DI-AMMONIUM HYDROGEN PHOSPHATE

Abeer F. ElHagrassy

Conservation Department, Faculty of Archaeology, Fayoum University, Egypt
(afa01@fayoum.edu.eg)

Received: 09/01/2024
Accepted: 29/01/2024

ABSTRACT

The objective of this study was to evaluate the efficiency and compatibility of two concentrations of di- ammonium hydrogen phosphate. Investigate the possibility of using it to consolidate the pigment layer of an Ancient Egyptian wooden coffin from the Middle Kingdom. X-Ray Diffraction (XRD), Fourier Transform Infrared Spectroscopy (FTIR), and Scanning Electron Microscope (SEM-EDX) were used to characterize the painted layer. Egyptian blue, Hematite, Goethite, and Carbon were mixed with Animal glue as a binding medium. To apply the consolidation treatment and evaluate its effects, replicas were created based on the characterization analysis. The goal in creating calcium phosphates is by using the two concentration treatments (0.1M and 1M) of a solution of diammonium hydrogen phosphate (DAP). Research findings indicated that the two concentration treatments may have increased the mechanical properties of the painted layer and caused acceptable color changes. The DAP (1M) treatment had a significant impact on water absorption, while the DAP (0.1M) treatment had a slight impact on those properties. The treated replicas (0.1M, 1M) displayed a higher drilling resistance compared to the untreated replica The high-water solubility, absence of toxicity, and low solubility of calcium phosphate make this consolidate very promising. The results show that the consolidating process is effective, there is no significant color change, and water absorption is reduced. The ammonium phosphate phase (hydroxyapatite) has the potential to be a highly promising agent for consolidating painted layer.

KEYWORDS: Di-hydrate ammonium phosphate, Hydroxyapatite, Consolidation, Coffin, Painted layer, Pigments, Conservation, FTIR, XRD, SEM-EDS, Goethite, Calcium phosphate.

1. INTRODUCTION

Every conservator worldwide faced the challenge of finding a way to control or delay the effects of deterioration and degradation processes. One of the most durable materials used in decorative historic buildings, tombs, coffins, and many other monuments is pigments (Ruolo, 2017). However, over time, weathering phenomena can seriously affect various decay processes leading to physical and chemical weathering of paint layers. (Siegesmund, 2002). Earlier analytical work for conservation purposes on Egyptian wooden coffin have been reported (Affifi et al., 2019; Abdelmoniem et al., 2020 a, b).

The mineral pigments are not suitable for consolidation with any of the commercially available consolidating products. It is typically divided into two categories, the organic polymeric products and the inorganic mineral products (Matteini, 2008).

The application process for these two types is different, with the organic polymeric products being ready to use after being dissolved in suitable organic solvents and applied with a brush. The polymers formed a film or blocked the pore space of the pigments after the solution penetrated the pores of the mineral pigments and the solvent evaporated causing the consolidating effect. (Vicini, 2001; Wheeler, 2005). Otherwise, inorganic mineral products are based on the chemical interaction with the pigments' mineral or their ground-based layer via carbonation or hydrolysis such as using of all based mineral nanoparticles (Alakbari, 2020).

Consolidation is not achieved by either the organic or inorganic consolidating products. The impeded movement of water vapour from the interior of the consolidated substrate towards the exterior can lead to enhanced deterioration of polymeric products. The penetration depth of inorganic products, including nanoparticles, is low (1 mm), Numerous studies have reported this, and it is not caused by the nanoparticles themselves, but rather by nanoparticles re-transporting towards the surface during drying. (Baglioni, 2015) (Rodriguez-Navarro, 2018).

A new treatment that utilizes ammonium oxalate has recently been proposed and applied as a consolidating treatment for plasters and carbonatic materials (Marino, 2007; Matteini, 2007). The mechanism of action is determined by the formation of micro-crystals of calcium oxalate (Ma, 2017; Sassoni, 2020), as described in the following equation:

$$(NH_4)_2C_2O_4 + CaCO_3 \rightarrow CaC_2O_4 + 2NH_3 + CO_2 + H_2O$$

The use of ammonium phosphates is another innovative approach that forms a mechanism similar to the one used in ammonium oxalate. The possible advantages offered by the ammonium phosphates are: (Sassoni, 2011; Naidu, 2011).

a: No toxicity (good point compared to nano-particles)

b: The solution has a higher concentration of the consolidating product.

c: Very low solubility of calcium phosphate (reactant).

Di-ammonium hydrogen phosphate (DAP) $(NH_4)2HPO_4$ is utilized to achieve the consolidation effect by forming hydroxyapatite (HAP) (Sassoni et al., 2013; 2016). The resulting product depends on the pH condition when DAP interacts with a calcareous substrate. For pH = 8, the chemical products are octacalcium phosphate (OCP) or hydroxyapatite (PAH) (Matteini M. R., 2011), according to the following reactions:

$$8CaCO_3 + 6(NH_4)2HPO_4 \rightarrow Ca_8(HPO_4)_2(PO_4)_4 + 12NH_3 + 8CO_2 + 8H_2O \quad \text{eq. 1}$$

$$10CaCO_3 + 6(NH_4)2HPO_4 \rightarrow Ca_{10}(PO_4)_6(OH)_2 + 12NH_3 + 10CO_2 + 8H_2O \quad \text{eq. 2}$$

The expected reaction products are Monetite (CHP), brushite (CHPD), and hydroxyapatite (HAP) if the pH is 5.6-6, as per the below reactions (Ugolotti, 2023):

$$CaCO_3 + (NH_4)H_2PO_4 \rightarrow CaHPO_4 + NH_3 + CO_2 + H_2O \quad \text{eq. 3}$$

$$CaCO_3 + (NH_4)H_2PO_4 + H_2O \rightarrow CaHPO_4.2H_2O + NH_3 + CO_2 \quad \text{eq. 4}$$

$$10CaCO_3 + 6(NH_4)H_2PO_4 \rightarrow Ca_{10}(PO_4)_6(OH)_2 + 6NH_3 + 10CO_2 + 8H_2O \quad \text{eq. 5}$$

The solubility isotherms expressed in a typical solubility phase diagram can be used to represent the stability of the hydroxyapatite phases in the form of log Ca+2tot graphs with respect to pH. (Chen, 2004) (Clark, 1955). It can be observed that increasing pH significantly decreases the solubility of HAP and TCP. (Brown, 1960).

The chemical composition and mass fraction are determined by pH during the formation of calcium phosphate at different stages (Wang, 2008). The triprotic equilibria of these systems affect the relative concentration of the four forms of phosphoric acid due to variations in pH. Calcium phosphate type and amount are formed by direct precipitation (Possenti, 2016).

The present study concerns a new treatment applied on pigments of Middle Kingdom wooden coffin from Helwan excavation area. The aim is to evaluate the efficacy and compatibility of using an aqueous solution of DAP and to evaluate the chemical, physical and color changes of coffin's pigments.

2. MATERIALS AND METHODS

2.1 Materials

The following materiuals were used: Di-ammonium hydrogen phosphate (DAP): manufactured in pioneer for chemicals (Piochem), Egypt. Assay 99%, Cas no: 7722-76-1; Ammonium phosphate (AP) manufactured in pioneer for chemicals (Piochem), Egypt. Assay 99%, Cas no: 7783-20-2; and, Ethyl Alcohol (EtOH): manufactured in pioneer for chemicals (Piochem), Egypt. Assay 95%, Cas no: 64-17-5.

Consolidants

Two concentrations of phosphate consolidation were utilized for this experiment, 1M DAP+ 30vol % of EtOH and 0.1M DAP+ 30vol % of EtOH as per previous studies (Sassoni, 2018a; Sassoni et al., 2018b).

Applying the consolidants onto the painted phase of a ground layer cube (5cm3) that had already been covered with painted layers (red, yellow, blue, and black) was done by brushing (10 strokes). Allow approximately 3 minutes of absorption between consecutive brushstrokes. To prevent evaporation, the replica was wrapped in a polyethylene sheet and left to react for 72 hours. For each consolidant/pigment, three cubes were treated.

2.2 Methods

Scanning Electron microscope

A SEM microscope was used to examine and analyze a painted layer. The EDX Unit attached to the SEM was used to obtain the micrographs obtained by Jeol JSM (5600 LV), Philips XL 30. The magnification range of the EDX Unit was from 10x to 400.000x, with a resolution of W is (3.5nm).

X- Ray Diffraction (XRD)

A Philips X-Ray Diffraction device model PW/1710 with Monochromator, Cu- radiation (λ=1.542A) at 40Kv, 30 MA and scan speed 0.02 /sec were used. The reflection peaks between 2=2 and 60 were determined with the corresponding spacing (d, A) and relative intensities (1/1). The ICDD files are compared with the diffraction graph and relative strengths obtained.

FTIR Spectroscopy

The Nicolet Nexus spectrophotometer (Washington, USA) and Nicolet Continuum were used to perform Fourier transform infrared (FTIR) analyses. A microscope with a HgCdTe detector cooled with liquid N2 that transforms infrared spectroscopy. Spectrums registered by a Graseby-Specac diamond cell accessory in transmission mode between 4000 and 700 cm^{-1}.

Spectrophotometer

Color –E Y E- 3100- Spectrophotometer – Basic User Manual, D L Company. Primary points were chosen to study the color change of mineral pigments. To determine the ΔE according to this equation, these points were measured both before and after consolidation.

Measurements were carried out before and after the consolidations. Color variation was determined by calculating the $\Delta E* = [(\Delta L^{*2}+\Delta a^{*2}+\Delta b^{*2})^{1/2}]$ where $\Delta L^* = L^*$ treated – L^* untreated, $a^* = a^*$ treated – a^* untreated, _b∗ = b^* treated – b^* untreated ($\Delta E^* = 5$ = human eye detection limit, HEDL). (L) indicates lightness (black & white), (a) is (green & red) coordinate, and (b) is (blue & yellow) coordinate.

Drilling Resistance

The DRMS was used to determine drill resistance in both treated and untreated replicas (Exadaktylos et al., 2000; Fratini et al., 2006). The diamond drill bit (Diaber) was used for drilling. At the optimal operating conditions, three holes were achieved for each measurement recognized for its ability to penetrate soft materials at a rate of 100 rpm/40 (mm/min) with a penetration depth of 10 mm.

Water Absorption

AA.VV. 2000 were used to measure the water uptake of untreated and processed replicates. The replicas were dried at 60◦c until constant weight (Wd = dry weight) (AA.VV., 2000). Deionized water was allowed to enter the replicate through the treated face, the samples replicas were weighed (Ww = wet weight) after 15, 30, 45, 60, 120, 180, 240, 360, 480, 600,720 min for both treated and untreated replicas. The absorption reduction (WAR%) was calculated according to the below equation:

WAR% = [(Ww − Wd) untreated − (Ww − Wd) treated] X 100 / (Ww − Wd) untreated

3. RESULTS

3.1 Painted Layers morphology and structure

After excavation and prior to any primary treatments, the painted layer fragments were taken from the excavated coffin for analysis and characterization.

Ground layer Structure

According to the XRD analysis, the ground layer is mainly composed of Gypsum ($CaSO_4.2H_2O$) at approximately 59.3%, Calcite $CaCO_3$ at approximately 33.6%, and traces of Quartz (SiO_2) at approximately 7.1% (Fig. 1).

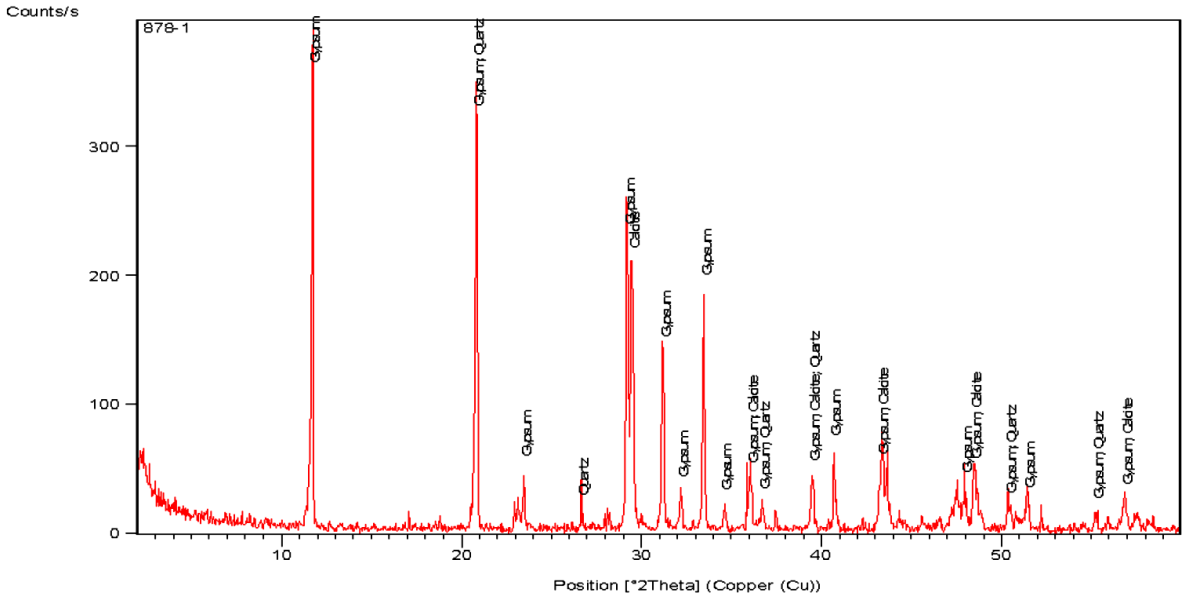

Figure 1. The XRD pattern showed the minerals that were present in the ground layer.

Painted layer

SEM-EDX analysis was performed on the fragments of the painted layer. The data demonstrated that the blue pigment is Egyptian blue ($CaCuSi_4O_{10}$) due to the represent of the elements (Cu, Ca, Si) (See SEM fine grains of the Egyptian blue, in Fig. 2).

In Fig. 3, the red pigment is Hematite (Fe_2O_3) due to the represent of the elements (Fe) while (Ca, Si) are ground layer elements, while in Fig. 4, the yellow pigment is Goethite (FeOOH) due to the represent of the elements (Fe) while (Ca, Si) are ground layer elements, and in Fig. 5, the black pigment is Carbon (C).

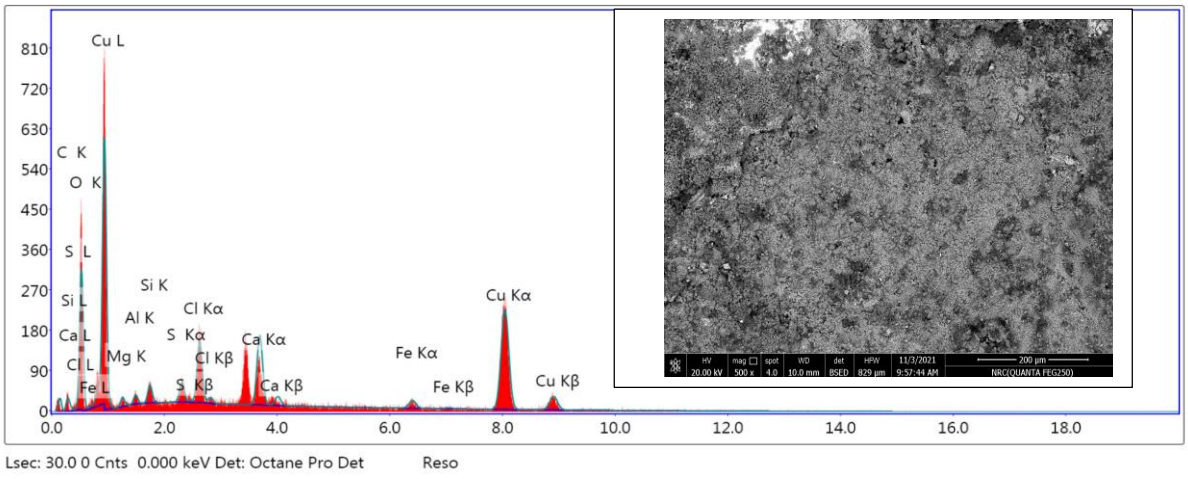

Figure 2. The SEM Morphology of the pigment (500x) and the EDX Spectrum analysis of Egyptian blue.

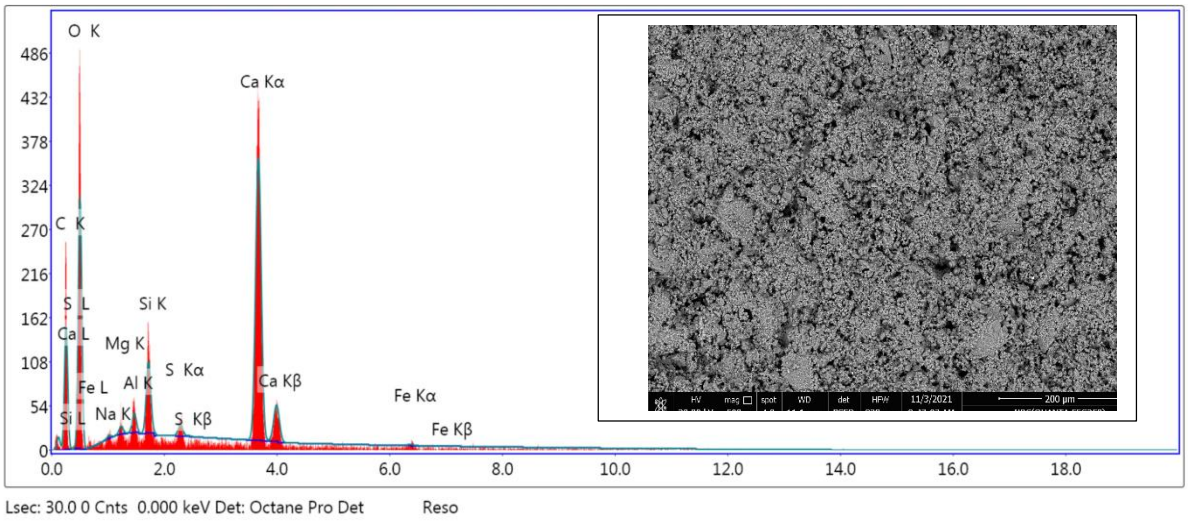

Figure 3. The EDX pattern analysis of the Hematite and the SEM Morphology of the pigment (500x).

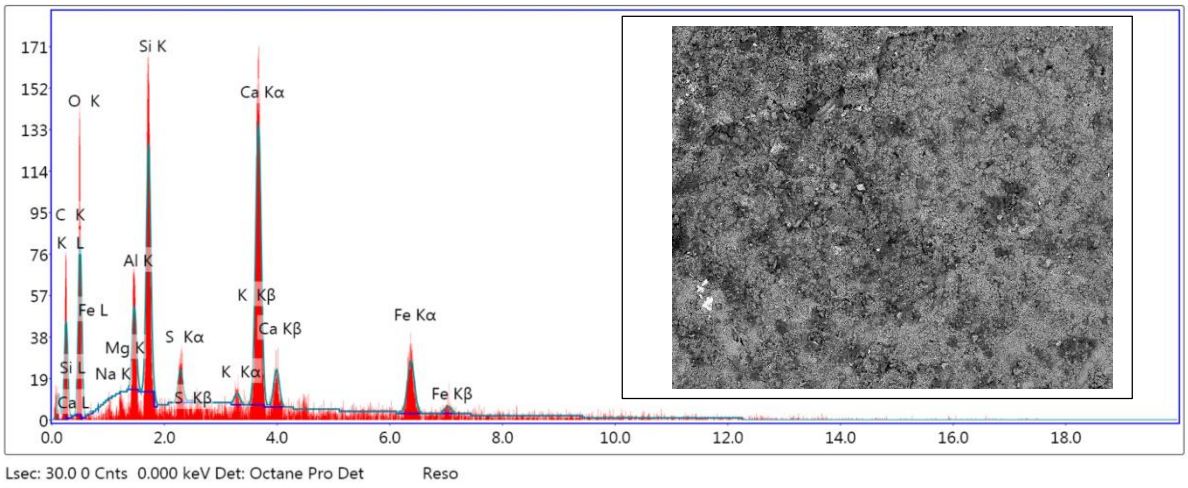

Figure 4. The EDX pattern analysis of the Goethite and the SEM Morphology of the pigment (500x).

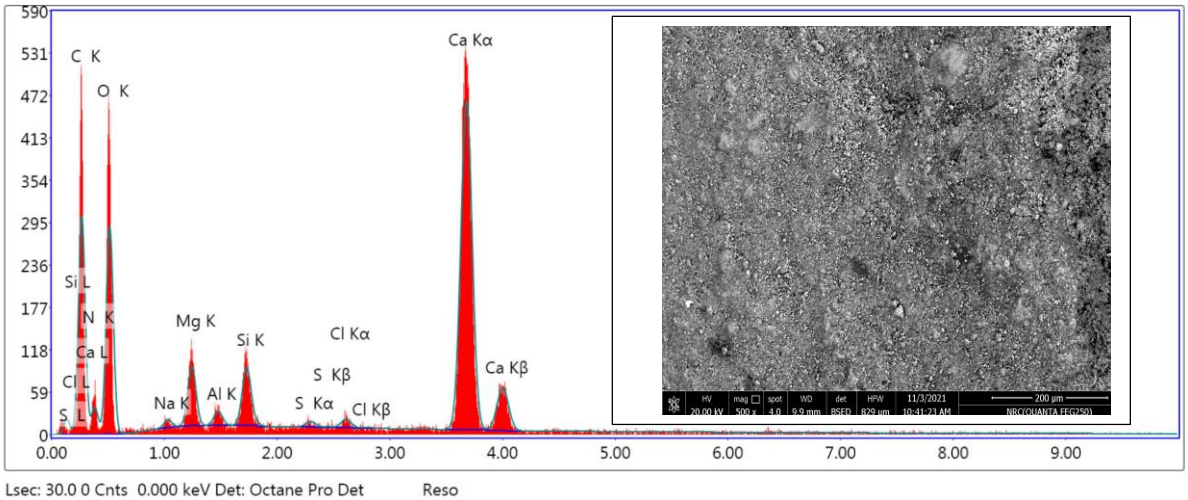

Figure 5. The EDX pattern analysis of the Carbon and the SEM Morphology of the pigment (500x).

Binding medium

A slight amount of animal glue was observed in the FTIR spectra as a binding medium. The activated group is present in the painted layer, which is characterized by it. The N-H stretching of $-CONH_2$ in the protein is the sharp peak at 3300–3430 cm^{-1}. The secondary amide protein (C=O) experiences a unique peak at 1640 cm^{-1}. (Fig. 6, Table 1) (Vahur et.al., 2016).

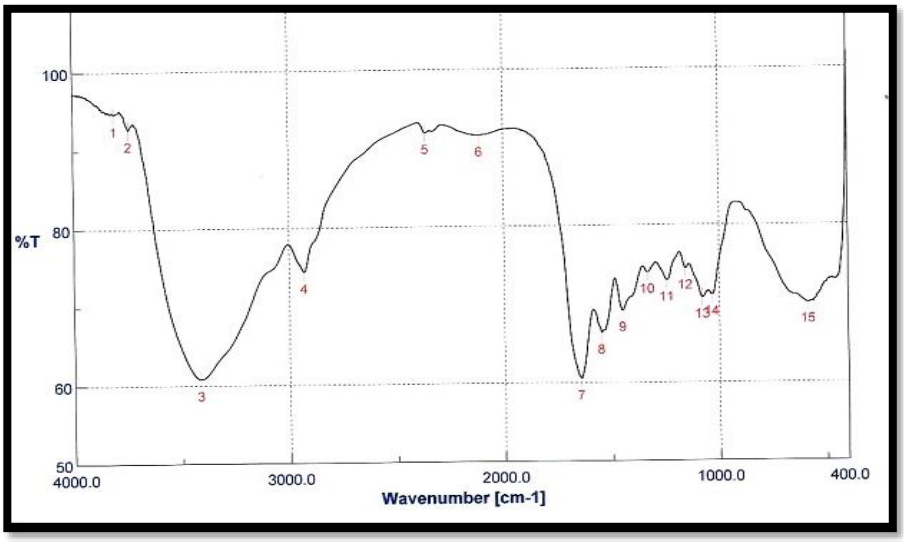

Figure 6. The pigment's binding medium is presented by the animal glue in the FTIR spectra (numbers in peaks see Table 1).

Table 1. The interpretation of the FTIR spectrum of the binding media.

No. In the Figure	Activated Group/ minerals	Wave Length (cm^{-1})
1, 2, 14, 15	Goethite (Yellow pigment)	3691,3651, 1078, 601
3	N-H	3394
4	C-H	2763
5, 6, 12, 13	Gypsum	2324, 2162, 1108, 1005
7	C=O	1721
8	CN-NH	1564
9, 10	$CaCO_3$	1420, 1322
11	C-OH	1326

Deterioration phenomena

During the study of the pigments, the painted layer was affected by two main deterioration phenomena. First, the micro-fissures are scattered on the pigments of the coffin. The dusty pigments are caused by heat and humidity and the loss of binding media (Figures 7 and 8).

Figure 7. The painted layer of the coffin is covered with micro-crakes.

Figure 8. The loss and dusting of pigments is due to the weakness of it.

The new phase consolidation layer's morphology and composition.

Both XRD and FTIR analysis were used to examine the treated and untreated replicas to determine the new composition of the new phase consolidated layer. The HAP layer is represented in the XRD and FTIR as shown in the oval shapes in Figs. 9 and 10 respectively. SEM is utilized to examine it morphologically as depicted in Fi.11 which shows the formation of the new crystals of HAP.

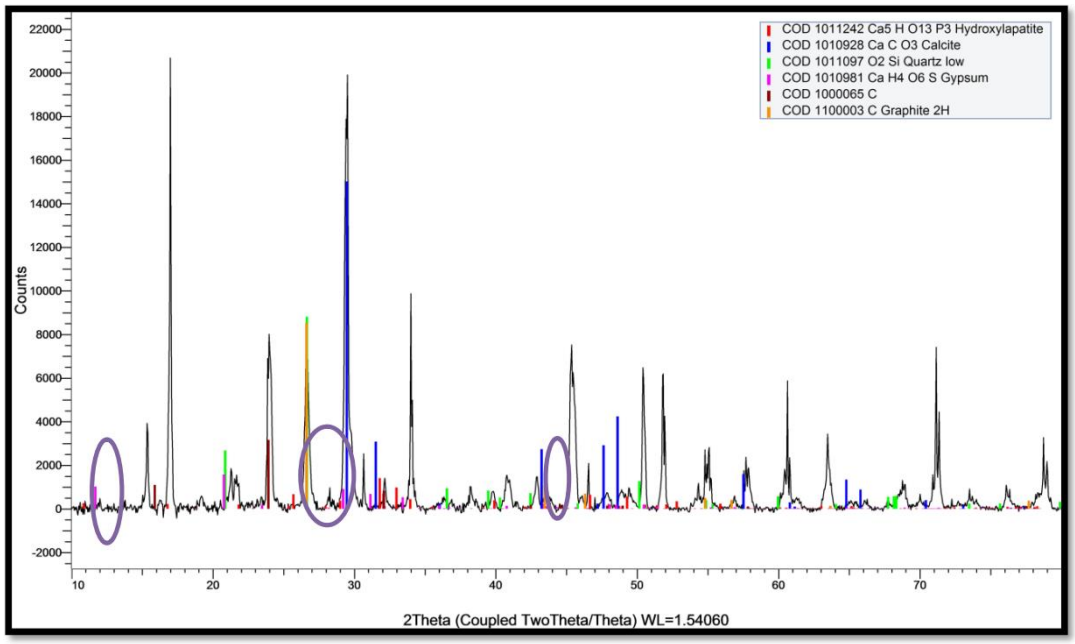

Figure 9. The XRD pattern of the calcium phosphate as a new consolidated phase. The HAP layer is shown in the oval shapes.

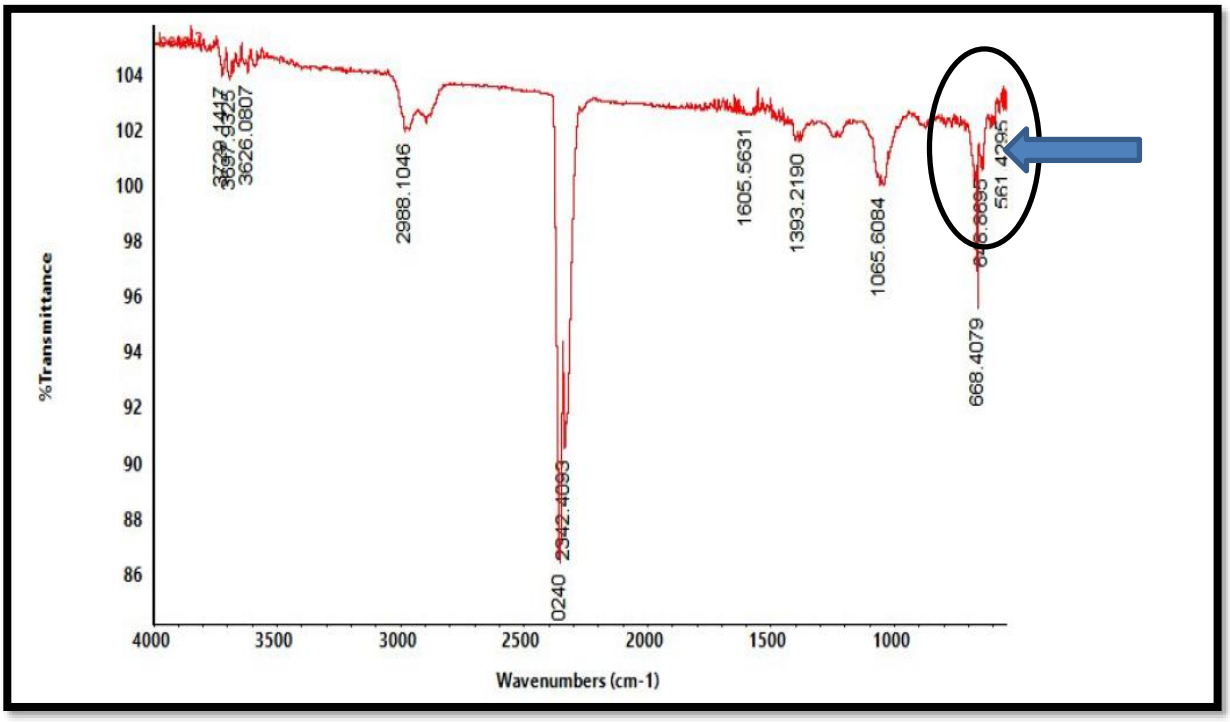

Figure 10. The FTIR pattern of the calcium phosphate. The HAP layer is shown in the oval shape.

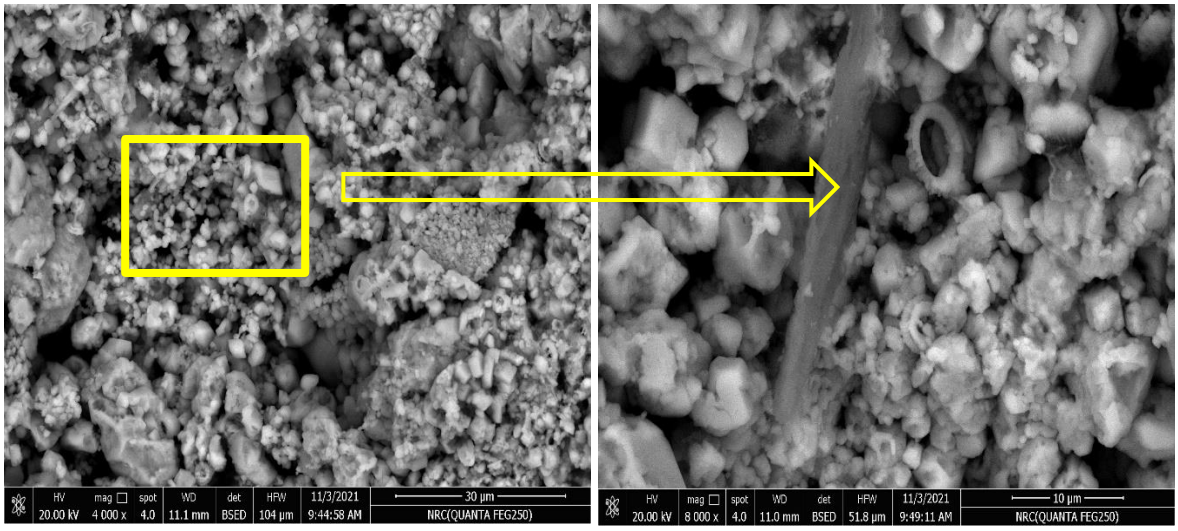

Figure 11. The Consolidated layer morphology (4000x, 8000x)

Color change by spectrophotometer

The color change (ΔE) assessment allowed to distinguish the differences between treated and untreated replicas and between each treatment concentration. The quantitative values of the outcomes for concentration 0.1M are displayed in Table 2, and for concentration 1M are displayed in Table 3.

Table 2. The ΔE of the painted layer before and after consolidation 0.1M DAP.

Pigments	Untreated			Treated with 0.1M			ΔE
	L*	a*	b*	L*	a*	b*	
Egyptian blue	-48.89	-42.07	50.17	-53.43	-41.12	53.08	2.78
Hematite	44.16	13.88	12.53	46.01	15.52	13.55	2.67
Goethite	54.72	7.98	24.23	56.66	8.07	25.81	2.50
Carbon	42.54	-18.36	19.71	44.55	-17.22	21.33	2.82

Table 3. The ΔE of the painted layer before and after consolidation 1M DAP.

Pigments	Untreated			Treated with 1M			ΔE
	L*	a*	b*	L*	a*	b*	
Egyptian blue	-48.89	-42.07	50.17	-53.35	-41.68	56.77	4.88
Hematite	44.16	13.88	12.53	47.13	17.15	13.96	4.64
Goethite	54.72	7.98	24.23	56.89	11.01	25.58	3.96
Carbon	42.54	-18.36	19.71	45.34	-19.42	23.03	4.21

Drilling Resistance

In two depth ranges, 0–20 mm and 0–5 mm, the drilling resistance was reported as an average value. The treated replicas (0.1M, 1M) displayed a higher drilling resistance compared to the untreated replica. (Table 4, 5). According to the SEM, a hard superficial layer with a concentration of 1M can be formed due to a high reactivity whereas the low reactivity allows the consolidation product to penetrate more deeply into the replicate (0.1 M) (Fig. 12).

Comparing the drilling data with the increase in contact time does not indicate an increase in drilling resistance for (DAP 1M). A noticeable increase in drilling resistance has been observed in the case of DAP (0.1M).

Table 4. The drilling resistance before and after consolidation DAP 0.1M.

	The drilling resistance (N)		
	Time (h.)	Force (0-5mm)	Force (0-20mm)
DAP 0.1M.	4	35.3	33.4
	6	36.9	34.7
	8	37.9	36.0
	10	38.6	37.5
	12	39.9	39.5
	24	40.3	39.9
Untreated		24.6	25.8

Table 5. The drilling resistance before and after consolidation DAP 1M.

	The drilling resistance (N)		
	Time (h.)	Force (0-5mm)	Force (0-20mm)
DAP 1M.	4	37.1	35.6
	6	37.5	36.3
	8	37.9	36.8
	10	37.9	36.9
	12	37.9	36.9
	24	37.9	36.9
Untreated		24.6	25.8

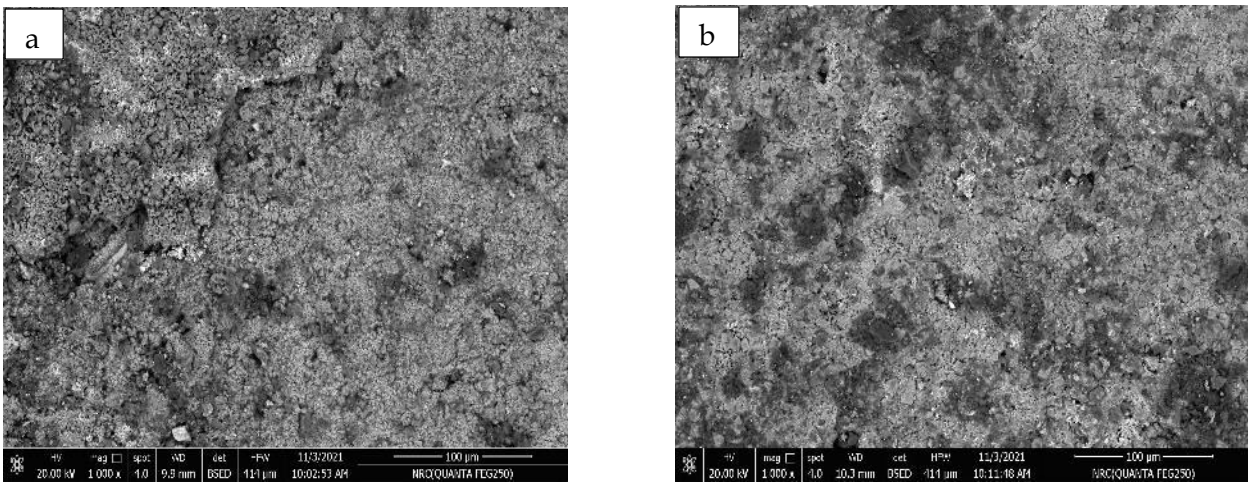

Figure 12. The Consolidated layer morphology (a: 0.1M, b: 1M) with magnification 1000x.

Water Absorption

The water absorption reduction (WAR%) (average 5.66%) did not experience any significant changes due to DAP (0.1M). The water intake of DAP (1M) decreased by approximately 11.39%, which was initially quite high and can hinder the size of the pores (Table 6).

Table 6. The water absorption reduction (WAR%) before and after consolidation DAP.

Time (min.)	The water absorption reduction (WAR%)	
	Treated with 0.1M	Treated with 1M
15	5.31	9.30
30	5.33	9.45
45	5.48	10.63
60	5.66	11.23
120	6.01	11.65
180	5. 77	11.98
240	5.79	12.01
360	5.78	12.32
480	5.78	12.30
600	5.71	12.30
720	5.71	12.30
Average	5.66	11.39

4. DISCUSSION

Fragments of pigments were taken from a Middle Kingdom ancient Egyptian coffin (2040 to 1782 BC) to conduct a characterization analysis. The artifact comes from the Helwan excavation area. Calcite, Gypsum, and quartz traces were determined by the XRD of the ground layer of the paintings. The EDX of the pigments revealed that the blue pigment was an ancient Egyptian blue, the red pigment was Hematite, and the coffin was covered with a light-yellow pigment made from Goethite mixed with Calcite. (Lucas, 1948).

The pigments were combined with a small amount of animal glue. According to the FT-IR spectra, the activated group, which is characterized by the N-H stretching of $–CONH_2$ in the protein, has a sharp peak at 3300–3430 cm^{-1}. The secondary amide protein (C=O) encounters a distinct peak in 1640 cm^{-1} binding media. (Nicholson, 2000)

In 2021, the coffin was excavated in Helwan, and it was completely covered with cracks. The painted layer is being lost due to its weakness and the high relative humidity of the atmospheric conditions, as well as the extreme UV index of temperature, which rises to 50°C.

The coffin's weakness necessitated a consolidation process. To consolidate these painted layers, Di-ammonium hydrogen phosphate (DAP) was utilized. Two concentrations of DAP in ethanol of 0.1M and 1M were created for consolidation. (Naidu, 2015). Ethanol has been discovered to enhance the densification of new calcium phosphates (Defus, 2021; Sassoni, 2018a, 2018b).

The untreated replica's SEM showed large pores in the calcite crystals. The ground layer surface showed the new calcium phosphates after DAP treatment, but they were not continuously coated with the new phases as in this case (Sassoni, 2018).

In carbonate material such as the ground layer of painted layer, new calcium phosphates formed by reacting with ammonium phosphate solutions typically have a flower-like morphology (Sassoni, 2018a) (Molina, 2018). The formation of small clusters has been reported in the case of lower concentration solutions in XRD spectrum represented (such as those used in the present case) (Sassoni et al., 2018b). At 602 and 561 cm^{-1}, small new bands appeared after DAP treatment,

which signified the formation of new calcium phosphates (Hydroxyapatite) as shown in the FTIR spectrum (Karampas, 2013).

To distinguish between the formation of hydroxyapatite and octa-calcium, which are both capable of being formed and both have FT-IR bands at 560–563 and 600–602 cm^{-1} (Naidu, 2014), It is important to consider the position of the other strong bands (at 1065 cm^{-1} for HAP and 1605 cm^{-1} for OCP). The strong band at 1080 cm^{-1} overlapped with the other band in the present case, resulting in no other bands being clearly visible due to quartz in the substrate (Dorozhkin, 2011).

Based on the measurement of the spectrophotometer. An increase in L* value was caused by the high concentration of DAP treatment, which resulted in some whitening and a shift towards blue due to the decrease in b* value. This outcome corresponds to what was evaluated in previous studies (Graziani, 2015; Shekofteh, 2019). The color shift was not higher than the commonly accepted threshold for conservation treatments (ΔE*=5) especially at low concentrations (ΔE*=3). In the event that DAP treatment is administered at a high concentration. The color changes were below the acceptable threshold that is typically experienced (Balonis-Sant et al., 2013).

The reduction in water absorption demonstrated that the movement of liquid water within the replica was not completely blocked after any concentration of consolidation. The consensus is that a consolidant should not drastically alter the water transport properties or prevent the exchange of water between the stone and the environment. DAP (0.1M) had a water absorption reduction that was 5.66 what could be considered low risk treatments. In contrast, DAP (1M) has increased by 11%, resulting in a moderate compatibility risk (Rodrigues, 2007).

The treated replicas (DAP 0.1M, 1M) displayed a higher drilling resistance compared to the untreated replica. This outcome protects the coffin from losing more pigments due to environmental conditions.

5. CONCLUSION

The purpose of this study is to evaluate the effectiveness and compatibility of two concentration DAP consolidants. None of the earlier research carried out on using this consolidation treatment on pigments. The research for first time demonstrates that the treatments based on ammonium phosphates applied to painted layer materials have a consolidating efficacy. At 0.1M DAP, the consolidating effect is generally more uniform than at 1M DAP. The rate of calcium phosphate formation at 0.1M is lower than it is at 1M, as indicated by this fact. The formation of fine crusts should be encouraged by this characteristic during 0.1M DAP consolidation, but it does not affect fine grains in 1M DAP.

According to the research, the color change after 0.1M and 1M DAP consolidation is generally less than the human eye's detection limit. With both concentrations, the water absorption capacity decreases in a systematic manner. The lower concentration has a higher decrease than the higher one. The drill resistance of the treated replicas (0.1M, 1M) was higher than that of the untreated replica. The consolidation product can penetrate more deeply into the replicate (0.1 M) thanks to a hard superficial layer with a concentration of 1M and low reactivity.

REFERENCES

AA.VV. (2000). *Determination of water absorption by capillarity.* UNI. Milan, Italy: UNI 10859.

Abdelmoniem M. A., Naglaa Mahmoud, Wael S. Mohamed (2020a) Isolation and characterization of microbial infection of polychrome wooden coffin from the 26th dynasty, Egypt. *SCIENTIFIC CULTURE*, Vol. 6, No. 3, 1-6. DOI: 10.5281/zenodo.3956802.

Abdelmoniem M. A., Naglaa Mahmoud, S.H. Samaha and Wael S. Mohamed (2020b) Characterization of the best consolidation material for black resin for the late period coffin. *SCIENTIFIC CULTURE*, Vol. 6, No. 1, 1-7. DOI: 10.5281/zenodo.3483979.

Afifi, H., Safa Abd El-Kader Mohamed Hamed, Samia Mohamedy, Michael Dawod (2019) A dating approach of a refundable wooden Egyptian coffin lid. *SCIENTIFIC CULTURE*, Vol. 5, No. 1, 15-22. DOI: 10.5281/zenodo.1451900.

Alakbari, F. S., Mohyaldinn , M.E., Muhsan, A.S., Hasan, N., Ganat, T. (2020). Chemical Sand Consolidation: From Polymers to Nanoparticles. *Polymers* 12, 1069.

Baglioni, P., Carretti, E., Chelazzi, D. (2015). Nanomaterials in art conservation. *Nat. Nanotechnology* 10, 287–290.

Balonis-Sant, M., Ma, X., Kakoulli, I (2013). Preliminary results on biomimetic methods based on soluble ammonium phosphate precursors for the consolidation of archaeological wall paintings, ACS Symp.

Ser. Archaeol. Chem., chapter 22, Washington, DC.: *ACS Symposium Series; American Chemical Society:* Washington, DC. 419–447.

Brown, W. (1960). Behavior of slightly soluble calcium phosphates as revealed by phase equilibrium calculations, *Soil Science* 90, 51–57.

Chen, Z.F., Darvell, B.W., Leung, V.W.H. (2004). Hydroxyapatite solubility in simple inorganic solutions. *Archives of Oral Biology* 49,359–367.

Clark, J. (1955). Solubility criteria for the existence of hydroxyapatite. *Canadian Journal of Chemistry* 33, 1696–1700.

Delgado Rodrigues and Grossi, 2007) Delgado Rodrigues J, Grossi A (2007) Indicators and ratings for the compatibility assessment of conservation actions. *J Cult. Herit*. 8:32–43. https://doi.org/10.1016/j.culher.2006.04.007

Defus, A., Possenti, A., Sansonetti, A., Tedeschi, C., Colombo, C., Biondelli, D., Vettori, S., Realini, M. (2021). Di-ammonium hydrogen phosphate for the consolidation of lime-based historic mortars – Preliminary research, *Journal of Cultural Heritage* 48, 45-53.

Dorozhkin, S. (2011). Calcium orthophosphates: Occurrence, properties, bio-mineralization, pathological calcification and biomimetic applications. *Biomatter*., 1, 121–164.

Exadaktylos, G.P.T & Filareto, C. (2000). Validation of rotary drilling of rocks with the drilling force measurement. I*nternational Journal of Restoration of Buildings and Monuments* 3, 307–340.

Fratini, F.S.R. & Tiano. P. (2006). A new portable system for determining the state of conservation of monumental stones. *Materials and Structures* 39,139–147.

Graziani, G., Sassoni, E., Franzoni, E. (2015). Consolidation of porous carbonate stones by an innovative phosphate treatment: Mechanical strengthening and physical-microstructural compatibility in comparison with TEOS-based treatments. *Herit. Sci*., 3, 1-6.

Karampas, I.A. & Kontoyannis, C.G. (2013). Characterization of calcium phosphates mixtures. *Spectroscopy* 64, 126–133.

Lucas, A. & harris, J.R. (1948). *Ancient Egyptian Materials and Industries*, Mineola, New York (Dover publication, INC.).

Ma, X., Balonis, M., Pasco, H., Toumazou, M., Counts, D., Kakoulli, I. (2017). Evaluation of hydroxyapatite effects for the consolidation of a Hellenistic-Roman rock-cut chamber tomb at Athienou-Malloura in Cyprus. *Construct. Build. Mater.* 150, 333–344.

Marino, A., Matteini, M., Fratini. F. (2007). Riflessioni critiche e nuove sperimentazioni sui trattamenti protettivi e consolidanti a base di ossalato di calcio artificiale. In: *Atti del XXIII Convegno di Studi su Scienza e Beni Culturali Il consolidamento degli apparati architettonici e decorativi*. Marghera: Italy, 99-108.

Matteini, M. (2008). Inorganic treatments for the consolidation and protection of stone artifacts. *Conserv. Sci. Cult. Herit.* 8, 13–27.

Matteini, M., Fratini, F., Rescic. S. (2007). Carbonate lithotypes passivated with the ammonium oxalate treatment: Colorimetric and morphological study of treated surfaces. *Science and Technology for Cultural Heritage* 16, 129–141.

Matteini, M., Rescic, S., Fratini, F., Botticelli, G. (2011). Ammonium Phosphates as Consolidating Agents for Carbonatic Stone Materials Used in Architecture and Cultural Heritage: Preliminary Research. *International Journal of Architectural Heritage*, 5, 717-736.

Molina, E., Fiol, C., Cultrone, G. (2018). Assessment of the efficacy of ethyl silicate and dibasic ammonium phosphate consolidants in improving the durability of two building sandstones from Andalusia (Spain). *Environ. Earth Sci.* 77, 302.

Naidu, S. & Scherer, G.W. (2014). Nucleation, growth and evolution of calcium phosphate films on calcite. *J. Colloid Interface Sci.* 435, 128–137.

Naidu, S., Liu, C., Scherer, G.W. (2015). Hydroxyapatite-based consolidant and the acceleration of hydrolysis of silicate-based consolidants. J*ournal of Cult. Herit. 1*6, 94–101.

Naidu, S., Sassoni, E., Scherer, G.W. (2011). New treatment for corrosion-resistant coatings for marble and consolidation of limestone. In: *Jardins de Pierres-Conservation of Stone in Parks, Gardens and Cemeteries;* Stefanaggi, M., Vergès-Belmin, V., Eds.; XL Print: Paris, France, 289–294.

Nicholson, P. & Shaw, I. (2000). *Ancient Egyptian Materials and Technology*. Cambridge University Press, UK.

Possenti, E., Colombo, C., Bersani, D., Bertasa, M., Botteon, A., Conti, C., Lottici, P.P., Realini, M. (2016). New insight on the interaction of di-ammonium hydrogen phosphate conservation treatment with carbonatic substrates: A multi-analytical approach. *Microchemical Journal* 127, 79-86.

Rodrigues, D & Grossi, J. A. (2007). Indicators and ratings for the compatibility assessment of conservation actions. *Journal of Cult. Heritage* 8, 32–43.

Rodriguez-Navarro, C., Ruiz-Agudo, E. (2018). Nanolimes: From synthesis to application. *Pure Applied Chemistry* 90, 523–550.

Ruolo, S.A., La Russa, M.F., Ricca, M., Belfiore, C.M., Macchia, A., Comite, V., Pezzino, A., Crisci, G.M. (2017). New insights on the consolidation of salt weathered limestone: The case study of Modica stone. *Bull. Eng. Geol. Environ.* 76, 11-20.

Sassoni, E. (2018a). Hydroxyapatite and Other Calcium Phosphates for the Conservation of Cultural Heritage: A Review. *Materials* 11, 557.

Sassoni, E. (2020). Lime and cement mortar consolidation by ammonium phosphate. *Construct. Build. Mater.* 245, 118409.

Sassoni, E., Franzoni, E., Pigino, B., Scherer, G.W., Naidu, S. (2013). Consolidation of calcareous and siliceous sandstones by hydroxyapatite: comparison with a TEOS-based consolidant. *Journal of Cultural Heritage* 14, 103-108.

Sassoni, E., Graziani, G., Scherer, G.W., Franzoni, E. (2016). Preliminary study on the use of ammonium phosphate for the conservation of marble-imitating gypsum-stuccoes. *Proceedings of the 4th Historic Mortars Conference HMC2016* (pp. 391-398). Santorini, Greece: A cura di: Papayianni, Ioanna ; Stefanidou, Maria ; Pachta, Vasiliki. ISBN 978-960-99922-3-7, Santorini, 391–398..

Sassoni, E., Graziani, G., Franzoni, E., Scherer, G.W. (2018b). Calcium phosphate coatings for marble conservation: Influence of ethanol and isopropanol addition to the precipitation medium on the coating microstructure and performance. *Corros. Sci*. 136,255-267.

Sassoni, E., Naidu, S., Scherer, G.W. (2011). The use of hydroxyapatite as a new inorganic consolidant for damaged carbonate stones. *Journal of Cultural Heritage*, 12, 346–355.

Shekofteh, A., Molina, M., Rueda-Quero, L., Arizzi, A., Cultrone, G. (2019). The efficiency of nanolime and dibasic ammonium phosphate in the consolidation of beige limestone from the Pasargadae World Heritage Site. Archaeol. Anthropol. Sci. 11, 5065- 5080.

Siegesmund, S., Weiss, T., Vollbrecht, A. (2002). *Natural Stone, Weathering Phenomena, Conservation Strategies and Case Studies.* London, UK.: Geological Society.

Ugolotti, G., & Sassoni, E. (2023). Effect of solvents and pH on in situ formation of hydroxyapatite for stone conservation. *Ceramics International,* 49, 14007-14016.

Vahur, S., Teearu, A., Peets, P. et al. (2016). ATR-FT-IR spectral collection of conservation materials in the extended region of 4000-80 cm^{-1}, *Analytical and Bioanalytical Chemistry* 408 (13), 3373–3379.

Vicini, S., Margutti, S., Moggi, G., Pedemonte, E. (2001). Pedemonte, E.In situ co-polymerisation of ethylmethacrylate and methylacrylate for the restoration of stone artefacts. *Journal of Cultural Heritage* 2, 143–147.

Wang, L. & Nancollas, G.H. (2008). Calcium orthophosphates: Crystallization and dissolution. *Chemical Reviews* 108,4628–4669.

Wheeler, G. (2005). *Alkoxy silanes and the consolidation of stone*. Los Angeles, CA: Getty Conservation Institute.